Drug Design, Development and Therapy

Dovepress
open access to scientific and medical research

Open Access Full Text Article

ORIGINAL RESEARCH

The load and release characteristics on a strong cationic ion-exchange fiber: kinetics, thermodynamics, and influences

This article was published in the following Dove Press journal:
Drug Design, Development and Therapy
16 July 2014
Number of times this article has been viewed

Jing Yuan
Yanan Gao
Xinyu Wang
Hongzhuo Liu
Xin Che
Lu Xu
Yang Yang
Qifang Wang
Yan Wang
Sanming Li

School of Pharmacy, Shenyang Pharmaceutical University, Shenyang, People's Republic of China

Abstract: Ion-exchange fibers were different from conventional ion-exchange resins in their non-cross-linked structure. The exchange was located on the surface of the framework, and the transport resistance reduced significantly, which might mean that the exchange is controlled by an ionic reaction instead of diffusion. Therefore, this work aimed to investigate the load and release characteristics of five model drugs with the strong cationic ion-exchange fiber ZB-1. Drugs were loaded using a batch process and released in United States Pharmacopoeia (USP) dissolution apparatus 2. Opposing exchange kinetics, suitable for the special structure of the fiber, were developed for describing the exchange process with the help of thermodynamics, which illustrated that the load was controlled by an ionic reaction. The molecular weight was the most important factor to influence the drug load and release rate. Strong alkalinity and rings in the molecular structures made the affinity between the drug and fiber strong, while logP did not cause any profound differences. The drug–fiber complexes exhibited sustained release. Different kinds and concentrations of counter ions or different amounts of drug–fiber complexes in the release medium affected the release behavior, while the pH value was independent of it. The groundwork for in-depth exploration and further application of ion-exchange fibers has been laid.

Keywords: ion-exchange fibers, ionic reaction, drug load and release, opposing exchange kinetics, thermodynamics, influences

Introduction

There has been growing concern on the delivery of active compounds, such as chemicals, peptides, or proteins, in a controlled manner. Each novel type of high-performance material guides researchers to a brand new field, including ion-exchange materials. Since the first synthesis of an ion-exchanger – ion-exchange resins in 1935[1] – ion-exchange materials that manifest specific functions, such as drug release based on the ionic environment, bio/mucoadhesive, and taste-masking, have provided an approach to novel drug delivery through adjusting and sustaining the release and permeation of drugs; it has been studied in oral,[2–5] transdermal,[6–9] mucosa,[10] and therapeutic embolic[11] drug delivery systems. Some ion-exchange resin complexes administrated orally that are already on the market, such as Delsym® (Reckitt Benckiser, Slough, UK), have illustrated that ion-exchange materials have important practical significance and broad application prospects.[12]

Ion-exchange fibers, as a typical type of ion-exchange material, contain two components: a water insoluble structural component (framework) consisting of polymer chains, such as polyethylene, polypropylene, or viscose, and a functional component

Correspondence: Sanming Li
School of Pharmacy, Shenyang Pharmaceutical University, Shenyang 110016, People's Republic of China
Tel +86 24 2398 6258
Fax +86 24 2398 6293
Email li_sanming@126.com

(exchange group) consisting of fixed negative (cationic exchanger) or positive (anionic exchanger) electric charges that are compensated by ions of the opposite charge, the so-called counter ions. The distinction between fibers and conventional resins is the non-cross-linked structure in the former.[1,13,14] Unlike the exchange between drugs and resins that happens in the pores and channels of resin particles, the exchange between drugs and fibers is located on the surface of the nonporous framework (Figure 1), and the transport resistance is reduced significantly, meaning the exchange is inclined to be controlled by an ionic reaction process instead of a diffusion process. Thus, a much faster loading rate and larger loading amount are possible because of a lack of pores and channels. These characteristics facilitate the preparation of drug–fiber complexes and improve patient compliance by markedly reducing the dose of materials.

A few kinetic theories based on diffusion have been developed for ion-exchange resins.[15,16] However, they are not suitable for fibers. Few studies have focused on the kinetics of drug loading into ion-exchange fibers. Chen et al[17] studied fibers that are composed of an inert hard core and a shell of ion-exchange material. The behavior of drugs diffusing into the inner film was the same as when they penetrated through the pores of resins. The mathematical treatment of ion-exchange processes in the fiber shell is similar to that in the conventional spherical resin, that is, the diffusion is the rate-determining process. Besides, precedents exist in the use of ionic reaction mechanisms to interpret the exchange processes of ion-exchange resins, particularly to those happening in ion-exchange columns.[1] However, because of the complex exchange processes and the cross-linked structure of resins, ionic reaction kinetics have obvious shortcomings.[18] But these kinetics might be a good choice for fibers because the exchanges happening on the surface of the non-cross-linked structure.

In this study, a novel type of kinetics based on the ionic reaction mechanism, named "opposing exchange kinetics", was developed to understand the nature and strength of interactions between drugs and fibers with the help of thermodynamics.

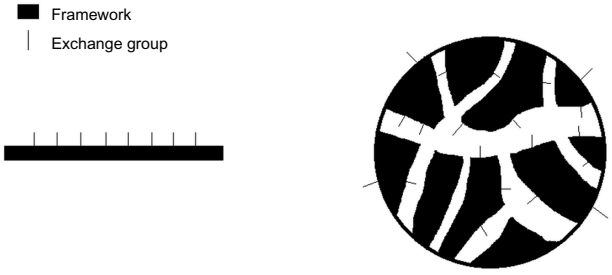

Figure 1 The distinction in structure between fiber (left) and resin (right).

The load and release behavior (rate and extent) of five model drugs in a strong cationic ion-exchange fiber (ZB-1) was investigated to learn how molecular weight, pKa (acid dissociation constant), logP, drug structure, and some other external conditions influence the load and release process.

Materials and methods

Materials

The strong cationic ion-exchange fiber ZB-1 used in this study was obtained from Guilin Zhenghan Co, Ltd, (Guangxi, People's Republic of China), with a maximum ion-exchange capacity of about 3.03 mmol/g and a diameter of 30–50 μm. The non-cross-linked framework of the fiber was polypropylene chain grafted with styrene side chains, and the strong cation-exchange group was sulfonic. Atenolol, diltiazem hydrochloride, sinomenine hydrochloride, tramadol hydrochloride, and venlafaxine hydrochloride were obtained from Wuhan Yuancheng Science and Technology Development Co, Ltd, (Hubei, People's Republic of China), Chengdu Geleixiya Chemical Technology Co, Ltd, (Sichuan, People's Republic of China), Shanghai Boshikai Chemical Science Co, Ltd, (Shanghai, People's Republic of China), Wuhan Yuancheng Science and Technology Development Co, Ltd., (Hubei, People's Republic of China), and Kerui-

Table 1 The structures, molecular weights, and physicochemical data of the model drugs

Drug (M_w)	Structural formula	pKa[a]	logP
Atenolol (266.34)	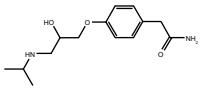	9.43±0.10	0.335±0.27[a]/ 0.5[b]/0.16[c]
Tramadol (263.38)	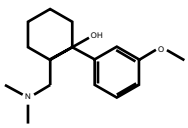	9.61±0.28	2.316±0.27[a]/ 2.4[b]/3.01[c]
Venlafaxine (277.40)	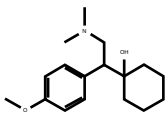	9.26±0.28	2.475±0.26[a]/ 2.8[b]/3.28[c]
Sinomenine (329.40)	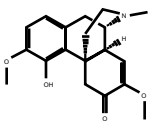	7.76±0.40	1.834±0.54[a]/ 1.05[c]
Diltiazem (414.53)	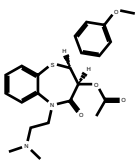	8.94±0.28	4.727±0.76[a] 2.8[b]/2.79[c]

Notes: [a]Data from https://scifinder.cas.org/; [b]data from http://www.drugbank.ca/; [c]data from http://www.syrres.com/what-we-do/databaseforms.aspx?id=386.
Abbreviations: M_w, molecular weight; pKa, the acid dissociation constant at a logarithmic scale.

Dekaihua Pharmacy Co, Ltd, (Sichuan, People's Republic of China), respectively. The structures, molecular weights, and physicochemical data of the model drugs are presented in Table 1. All the other chemicals were of analytical grade and were used without further purification. Self-prepared deionized water with a resistivity of more than 18 MΩ/cm was used to prepare all the solutions.

Methods

Pretreatment of the ion-exchange fibers

The fibers in staple form were washed consecutively by 95% ethanol and deionized water to remove impurities until the washing solution became colorless, and were then activated by recycling them between the basic and acidic forms with 0.01 M NaOH and 0.01 M HCl solutions, respectively, until the pH value of the washing solutions was stable at about 12 or 2. After washing with deionized water until neutral, fibers were immersed in 1 M NaCl solution several times in order to pre-load them with sodium ions. When the pH of the fiber pulp was nearly neutral, fibers were immersed in 1 M NaCl solution several times in order to pre-load them with sodium ions until the pH of the fiber pulp was nearly neutral, meaning that hydrogen ions bound on the fibers were replaced thoroughly by sodium ions. Finally surplus ions were washed away before the fibers were dried.[5] Before use, the fibers were cut into small units fine enough to pass through an 80-mesh screen.

Drug-loaded ion-exchange fibers

The drugs were loaded into the fibers using a batch process, whereby the previously purified fiber powders (100 mg dry weight) were immersed in a 3.5 mM solution of the drug (100 mL). Equimolar HCl was added into atenolol solution beforehand in order to ensure the drug remained in its cationic form. All the experiments were performed at a predetermined temperature in glass containers with a suitable volume placed in a thermostat water bath with continuous stirring at 500 rpm using a magnetic stirrer. Samples were collected through a 400-mesh filter screen from the drug–fiber system at designated time points, and then the same volume of water was added back into the system in order to maintain a constant volume. The amount of drug loaded onto the fibers was determined as the difference between the amount of drug in the initial loading solutions and samples. Each experiment was performed at least in triplicate.

Morphology of ion-exchange fibers

The surface characteristic of ion-exchange fibers was evaluated by scanning electron microscopy (SURA 35; Carl Zeiss AG, Jena, Germany). Samples were gold-plated using double-sided adhesive tape prior to imaging at 15.00 kV.

Drug release from ion-exchange fibers

The drug–fiber complexes (equivalent to 100 mg of atenolol, 100 mg of tramadol hydrochloride, 75 mg of venlafaxine hydrochloride, 60 mg of sinomenine hydrochloride, and 30 mg of diltiazem hydrochloride, respectively) were transferred to 900 mL of dissolution medium pH 1.2 HCl solution and pH 6.8 phosphate buffer in United States Pharmacopoeia (USP) dissolution apparatus 2 (RC-6 dissolution tester, Tianjin Optical Instrument Factory, Tianjin, People's Republic of China). The temperature of the medium was maintained at 37.0°C±0.5°C. The paddle was rotated at 50 rpm. All experiments were performed in triplicate.

Analysis of drug concentrations

The content of drug in the solutions was measured with a UV-Vis (ultraviolet-visible) spectrophotometer (UV-9100; Beijing Ruili, Beijing, People's Republic of China) at wavelengths of 273 nm, 271 nm, 273 nm, 265 nm, and 237 nm for atenolol, tramadol hydrochloride, venlafaxine hydrochloride, sinomenine hydrochloride, and diltiazem hydrochloride, respectively.

Statistical analysis

One-way analysis of variance was used to determine the significance among groups, after which post hoc tests with the least significant difference were used for comparison between individual groups. $P<0.05$ was considered as statistically significant.

Theory

Opposing exchange kinetics has been developed to describe the reversible ionic reaction that ion-exchange fibers undergo when placed in contact with a solution of ions. The load and release are simultaneous and the equilibrium will be reached when the positive and negative reaction rates are equal.

This type of ion-exchange reaction can be represented as follow:

$$RNa + DHCl \underset{k_2}{\overset{k_1}{\rightleftharpoons}} RHD + NaCl \quad (1)$$

where R and D stand for the ion-exchange fiber and the drug, respectively; k_1 and k_2 are the load and release rate constants. Here, NaCl is also considered to be a product due to its imperative role in the negative reaction, which is usually overlooked.[19,20]

The calculated rate of drug load at time t, as described by Equation 1, is given by:

$$r_c = \frac{dQ_t}{dt} = k_1(Q_0 - Q_t)^{\alpha}(Q_m - Q_t)^{\beta} - k_2 Q_t^{\gamma+\delta} \quad (2)$$

where Q_0 is the initial concentration (mmol/L) of the drug solution, Q_m is the maximum loading capacity (mmol/g) of the fiber, and Q_t is the loading amount (mmol/g) at time t. For an ion-exchange reaction, the positive and negative reaction rates are usually both proportional to one power of the concentrations of their reactants; therefore, the values of α, β, γ, and δ are 1:

$$r_c = k_1(Q_0 - Q_t)(Q_m - Q_t) - k_2 Q_t^2 \quad (3)$$

Among k_1, k_2, and the equilibrium constant K, there is a relationship:

$$\frac{k_1}{k_2} = K = \frac{Q_e^2}{(Q_0 - Q_e)(Q_m - Q_e)} \quad (4)$$

where Q_e refers to the equilibrium loading amount (mmol/g). In Equation 3, k_2 is substituted by k_1:

$$r_c = k_1 \frac{Q_e^2(Q_0 - Q_t)(Q_m - Q_t) - Q_t^2(Q_0 - Q_e)(Q_m - Q_e)}{Q_e^2} \quad (5)$$

Here, the ion exchange closely resembled the monomolecular layer adsorption in reversibility, which leads to a similarity in shape between the loading curve and the Langmuir adsorption isotherm curve. Therefore, an equation analogous to the Langmuir adsorption isotherm equation is used to get r_e, the measured reaction rate at time t, by fitting the points of Q_t versus t received from experiments:

$$Q_t = \frac{Q_e b t}{1 + b t} \quad (6)$$

$$r_e = \frac{dQ_t}{dt} = \frac{Q_e b}{(1 + bt)^2} \quad (7)$$

where b is the exchange coefficient.

Finally, k_1 is determined by the least squares method according to Equation 8:

$$\frac{d\Sigma_{i=1}^{t}(r_{ei} - r_{ci})^2}{dk_1} = 0 \quad (8)$$

In particular, the first and the last time points were not included in the calculation of the reaction rate since the end points of a bounded function are non-derivable.

The positive and negative reaction activation energies, E_{a1} and E_{a2}, respectively, can be calculated by the differential form of the "Arrhenius equation":

$$\ln k = -\frac{E_a}{RT} + C \quad (9)$$

The thermodynamic parameters: standard free energy change (ΔG^0), enthalpy change (ΔH^0), and entropy change (ΔS^0) were evaluated to test the feasibility, heat effect, and mechanism of the loading process.[21] All of them were related to the equilibrium constant K by the following equations:

$$\Delta G^0 = -RT \ln K \quad (10)$$

$$\ln K = -\frac{\Delta H^0}{RT} + \frac{\Delta S^0}{R} \quad (11)$$

Results and discussion

Drug-loaded ion-exchange fibers

Kinetics and thermodynamics

Figure 2 shows two types of curves of model drugs loading into the ion-exchange fibers at 25°C. Type one exhibited a very fast loading rate – 30 minutes was enough to reach equilibrium, while the loading amount was small, and the drugs included atenolol, tramadol, and venlafaxine; type two exhibited a slow loading rate – several days were needed to reach equilibrium, while the loading amount was larger, and the drugs included sinomenine and diltiazem. Opposing exchange kinetics captured the characteristics of the loading curves of atenolol and sinomenine, at three different temperatures, quite successfully (Figure 3), illustrating that the model could

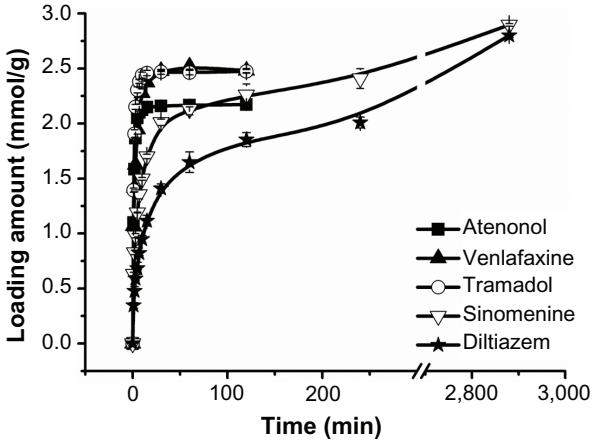

Figure 2 The loading curves of model drugs into ZB-1 at 25°C.

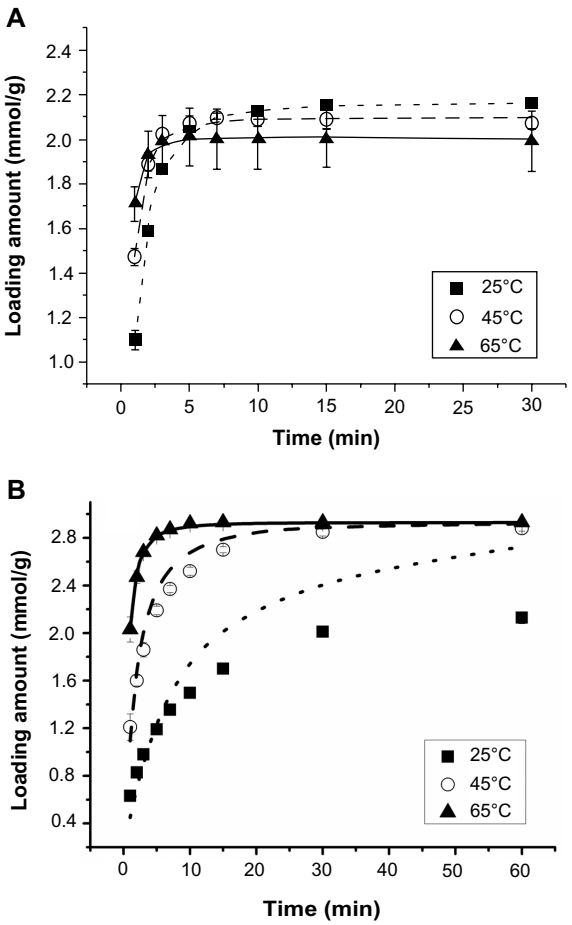

Figure 3 Measured values (points) and opposing exchange kinetics fitting curves of atenolol load (**A**) and the first 60 minutes of sinomenine load (**B**).
Note: The temperatures of experiments were 25°C (■, dot), 45°C (○, dash), and 65°C (▲, solid), respectively.

interpret the loading behaviors. Table 2 depicts the comparison between the experimental results (Q_t) and the theoretical predictions (Q_p) for atenolol at varying temperatures. The residual variations were small between the rates of ion-exchange and ionic reaction, suggesting that the ionic reaction was the rate-determining step for the loading process of ion-exchange fibers. However, for type two drugs at low temperature, the calculated values were somewhat higher than the observed ones, illustrating that there were other factors influencing the exchange rate under some conditions.

Theoretical considerations indicate that the rate constant should depend on the concentration of the reactants, with the exception of reactions between ions. By far the most dramatic effect on rate constants is caused by temperature changes.[22] The calculated rate constants of all the drug loads were increased as the temperature rose (Table 3) and did not depend on the initial concentrations of reactants at a certain temperature (results not shown). These results were in agreement with the general principles of kinetic theory.

The absolute of ΔG^0 shown in Table 4 was small, which meant that the direction of spontaneous reaction could not be determined, and the difference between the E_{a1} and E_{a2} of one drug shown in Table 3 was small. Both of them were characteristic of reversible reactions.

The results of ΔS^0 could provide some information on the ion-exchange mechanism. This value should be positive in an ionic reaction because the randomness in the (solid + liquid) interface is increased, attributed to the release of sodium and chlorine ions, which have a smaller radius; meanwhile, the value of the adsorption process should be negative due to the decrease in the particle number. In Table 4, the ΔS^0 for atenolol was negative, while that for the other four hydrochlorides was positive, which might suggest that the exchange of atenolol in ion-exchange fibers is apt to physical adsorption, while the others are more apt to ion reactions. High linearity is shown in Figure 4, in which the positive and negative reaction activation energies were calculated from the slope of ln$k$ versus $1/T$. Wang et al pointed out that the value of E_a depicted the type of adsorption: when its value is between

Table 2 Estimation of fitting accuracy of atenolol load at three temperatures

Time (min)	25°C			45°C			65°C		
	Q_t	Q_p (mmol/g)	R	Q_t	Q_p (mmol/g)	R	Q_t	Q_p (mmol/g)	R
1	1.10	1.07	0.03	1.47	1.48	−0.01	1.71	1.71	0.00
2	1.58	1.66	−0.08	1.89	1.88	0.01	1.93	1.92	0.01
3	1.87	1.88	−0.01	2.02	1.99	0.03	1.99	1.97	0.02
5	2.05	2.04	0.01	2.07	2.06	0.01	2.01	1.99	0.02
7	2.10	2.10	0.00	2.10	2.08	0.02	2.00	2.00	0.00
10	2.12	2.13	−0.01	2.09	2.09	0.00	2.00	2.01	−0.01
15	2.15	2.15	0.00	2.09	2.09	−0.00	2.00	2.01	−0.01
30	2.16	2.17	−0.01	2.07	2.10	−0.03	1.99	2.01	−0.02
RSS $\times 10^3$	7.7			2.5			1.5		

Note: Unit of measurement: mmol/g.
Abbreviations: R, residual; RSS, residual sum of squares; Q_t, experimental loading amount; Q_p, theoretical loading amount.

Table 3 Kinetics parameters calculated by opposing exchange kinetics for model drug loading experiments

Drug	Temperature (K)	Q_e (mmol/g)	k_1	E_{a1} (kJ/mol)	k_2	E_{a2} (kJ/mol)	K
Atenolol	298.15	2.17±0.02	0.135	7.6	2.41×10^{-2}	17.4	5.62
	318.15	2.10±0.02	0.170		3.95×10^{-2}		4.36
	338.15	2.01±0.13	0.194		5.53×10^{-2}		3.53
Tramadol	298.15	2.46±0.02	0.175	10.1	1.61×10^{-2}	13.9	10.9
	318.15	2.43±0.02	0.227		2.27×10^{-2}		9.9
	338.15	2.41±0.01	0.283		3.09×10^{-2}		9.1
Venlafaxine	298.15	2.52±0.02	0.117	20.8	7.79×10^{-3}	13.3	14.6
	318.15	2.56±0.01	0.240		1.32×10^{-2}		18.5
	338.15	2.61±0.01	0.313		1.55×10^{-2}		20.9
Sinomenine	298.15	2.90±0.02	3.37×10^{-2}	52.5	2.97×10^{-4}	43.9	1.14×10^{2}
	318.15	2.93±0.01	0.154		9.0×10^{-4}		1.72×10^{2}
	338.15	2.93±0.00	0.414		2.41×10^{-3}		1.72×10^{2}
Diltiazem	298.15	2.80±0.02	9.9×10^{-3}	69.0	2.21×10^{-4}	31.6	45.3
	318.15	2.92±0.03	5.70×10^{-2}		4.92×10^{-4}		1.16×10^{2}
	338.15	3.13±0.02	0.269		–		–

8 and 16 kJ/mol, it is a chemisorption, while it is a physisorption process when E_a is lower than –40 kJ/mol.[23] Nollet et al also reported that low activation energies (5–40 kJ/mol) are characteristic for physisorption, while higher activation energies (40–800 kJ/mol) suggest chemisorptions.[24] The E_{a1} of atenolol was below 8 kJ/mol, while the E_{a1} for the other drugs were all above it. The positive center of atenolol is a secondary amine while the others are tertiary amines. The secondary amine is much harder to ionize in solutions than the tertiary amine, so a coordination complex might be formed between it and hydrochloric acid instead of the ionic compound, resulting in atenolol being absorbed in the molecular form. Similarly, Borodkin et al[25] reported that greater affinity existed between the resin and tertiary amines than with secondary amines.

Table 4 Thermodynamic parameters of model drug loading experiments

Drugs	Temperature (K)	K	ΔG^0 (kJ/mol)	ΔH^0 (kJ/mol)	ΔS^0 (J/[K·mol])
Atenonol	298.15	5.62	–1.35	–9.75	–18.37
	318.15	4.36	–1.02		
	338.15	3.53	–0.65		
Tramadol	298.15	10.94	–2.16	–3.80	7.14
	318.15	9.87	–2.19		
	338.15	9.13	–2.23		
Venlafaxine	298.15	14.62	–2.44	7.51	47.59
	318.15	18.46	–2.83		
	338.15	20.88	–3.12		
Sinomenine	298.15	114.48	–3.86	8.67	68.99
	318.15	171.88	–4.33		
	338.15	171.78	–4.61		
Diltiazem	298.15	45.25	–3.32	37.07	156.03
	318.15	115.85	–4.12		

The results of ΔH^0 are also shown in Table 4. The exchanges for atenolol and tramadol are exothermic, which makes their load easier and K went down as the temperature increased; high temperatures benefit the negative reaction to obtain a smaller amount. For other endothermic reactions, K increased as the temperature rose; high temperatures benefit the positive reaction to obtain a larger loading amount. However, the effect of temperature on the loading amount was not statistically significant for atenolol and sinomenine ($P>0.05$), and statistically significant for tramadol, venlafaxine, and diltiazem ($P<0.05$).

Influences on loading drugs

The effect of model drug loading into ion-exchange fibers was investigated under the same initial molar concentration of reactants. The differences among the five drugs were tested in terms of four factors: molecular weight, pKa, logP, and the structural framework of the drug.

Molecular weight

The relationships of $\ln k_1$ or E_{a1} versus molecular weight are exhibited in Figure 5. The activation energy increased and loading rate decreased with increasing molecular weight. Good linearity adequately proved that molecular weight was the most important influence on drug load. The surface of the fibers where the ionic reactions occurred was limited unlike homogeneous reactions; thus, steric hindrance appeared to be a noticeable factor in affecting the loading process. While some parts of the drug ions bonded quickly with the ion-exchange groups, other parts needed more time to rearrange into an appropriate position for the exchange, typically for drug ions with larger molecule weights, which move more slowly. This is why the observed values of the

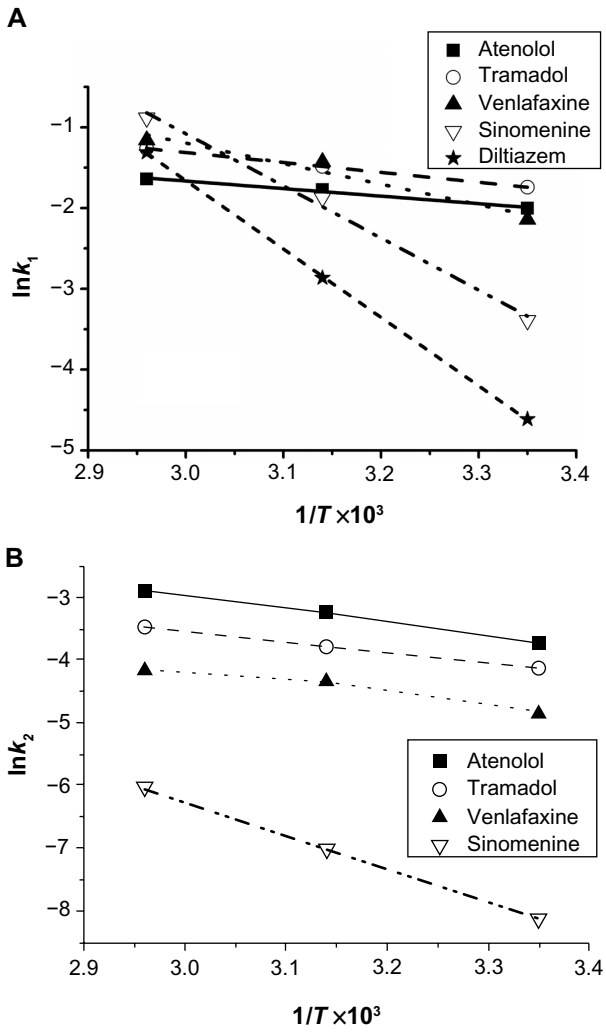

Figure 4 $\ln k_1$ (**A**) and $\ln k_2$ (**B**) versus $1/T$ for estimating the positive reaction and negative reaction.
Abbreviation: T, temperature.

exchange rate were somewhat lower than the predicted rates for sinomenine at lower temperatures. When the load occurred at a higher temperature, the time was shorter because of the acceleration of molecular thermal motion; the loading curve was similar to that of type one (Figure 2B).

pKa

As an ionic reaction in nature, since the negative electric charges of the exchange groups were definite, the charge density of the model drugs might impact on loading behavior,[26] that is, drug alkalinity. The molecular weight of tramadol and atenolol were nearly the same, but the pKa of the former was larger, which enhanced the affinity between the drug and the fiber, that made the load faster.

logP

The differences of logP among the drugs did not cause any profound differences in the load amount. In a previous study,

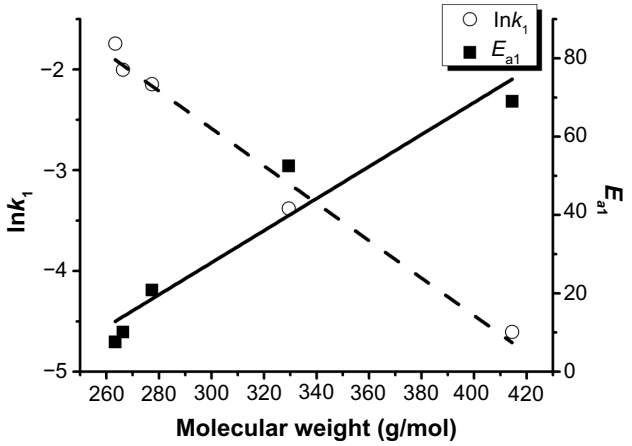

Figure 5 $\ln k_1$ versus molecular weight at 25°C, plotted with the molecular weight of model drugs loading.

Hänninen et al[13] also found similar results in the Smopex® DS-218v fiber (Johnson Matthey, Royston, UK).

Framework of drug structure

Helfferich noted that, "The ion exchanger prefers counter ions with organic groups which resemble the components of the matrix. For example, resins usually prefer counter ions with aromatic groups to those with aliphatic groups".[1,27] Here, more attention was paid on the framework of the drug structures, not on logP. The loading amounts in this study were increased notably ($P<0.05$) as the ring number increased. At 25°C, the loading amount for atenolol, with one ring in its structure, was the lowest (2.17 mmol/g), while that for sinomenine, which comprises four rings, was the highest (2.90 mmol/g). Rings in molecular structures strengthen the affinity between the drug and the fiber.

Morphology of ion-exchange fibers

The scanning electron micrographs of the ion-exchange fibers are shown in Figure 6. The surface of ZB-1 was composed of countless etched bulges. After being loaded, firstly, the crystals of the drug disappeared, ie, the drug in the fiber was in the amorphous state; secondly, the fiber surface became smoother due to the drug film covering it.

Drug release from ion-exchange fibers

The in vitro release of the five drugs from the ion-exchange fibers was studied by carrying out their dissolution in USP dissolution apparatus 2. The drug–fiber complexes were initially floated onto the surface of water due to their hydrophobicity and gradually sank after more than 6 hours. The floating ability could prolong the gastric retention time of complexes. The influences on drug release were investigated

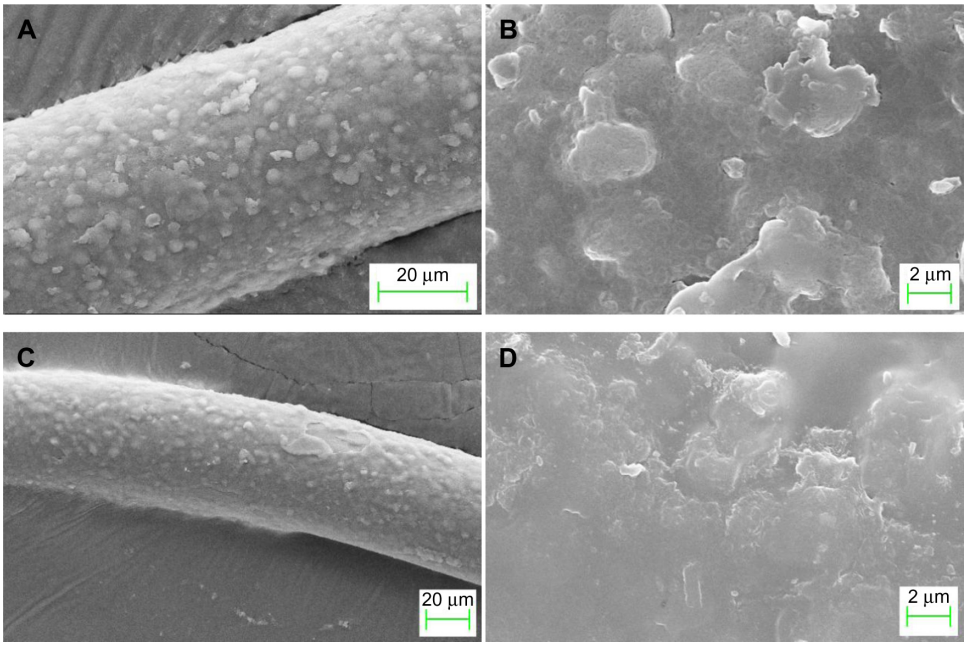

Figure 6 Scanning electron micrographs of ZB-1 (**A, B**) and Atenolol-fiber complexes (**C, D**) with different amplified times.

from two aspects: physicochemical properties and external conditions.

Molecular weight and pKa

The release profiles of each drug from the drug–fiber complexes in pH 1.2 HCl solution and pH 6.8 phosphate buffer are shown in Figure 7. The rate of drug release from the fiber was determined by extrapolating the time when 50% ($t_{50\%}$) and 80% ($t_{80\%}$) of the drug in the fiber was released into the dissolution medium (Table 5). Generally, the release rate decreased with increasing molecular weight. Atenolol was released very quickly from the fiber complexes, and the release rate was approximately the same as that of drug powder in pH 1.2 solution, and even faster than that of drug powder in pH 6.8 buffer. Atenolol-fiber complexes preformed an ability of rapid release. The reason for this is that the dissolving rate of atenolol powder is slow due to its strong surface hydrophobicity and comparatively low solubility; however, the highly dispersed state of the drug in the fiber accelerated the release. The other drug–fiber complexes exhibited sustained release, and the extent of this release increased as the molecular weight increased. Steric hindrance made it difficult for the extraction ions to approach the ionic bonds between the small ion-exchange groups and the much larger drug. Meantime, the release rate of tramadol was slower than that of atenolol, illustrating that the stronger affinity caused by higher charge density and ring structure between tramadol and the fiber made it harder to release. In oral administration, additional release control through another method, such as coating, is needed for ion-exchange resins.

External conditions

The release profiles for venlafaxine hydrochloride from the fiber complexes under various external conditions are shown in Figure 8. Different kinds and concentrations of counter ions in the release medium affect the release behavior, while the pH value is independent of it once the concentrations of counter ions in solutions are adjusted by NaCl. The order of the extent of release for the five extraction ions was $Ca^{2+} > Mg^{2+} > K^{+} > Na^{+} > H^{+}$. Although each kind of ion has its own special affinity for the ion-exchange fibers, the ability of the divalent ions is about one time greater than that for the monovalent ions, illustrating that the ion exchange is a stoichiometric reaction. When the molar amount of sodium ions was equal, ten-fold, or hundred-fold as compared to the drug ions in the fiber, the release percentages of the drug from the fiber were 17%, 46%, and 81%, respectively. The reason for this is that the increase in the molar amount of counter ions shifts the equilibrium toward drug release. Similarly, the release extent could also become higher as the solution volume increases. Prabhu et al[28] reported that the release of diltiazem hydrochloride from resinates is about 40% in pH 1.2 solution in the same apparatus. In comparison, in our work, the release of the drugs from the complexes was more than 80%. The drug

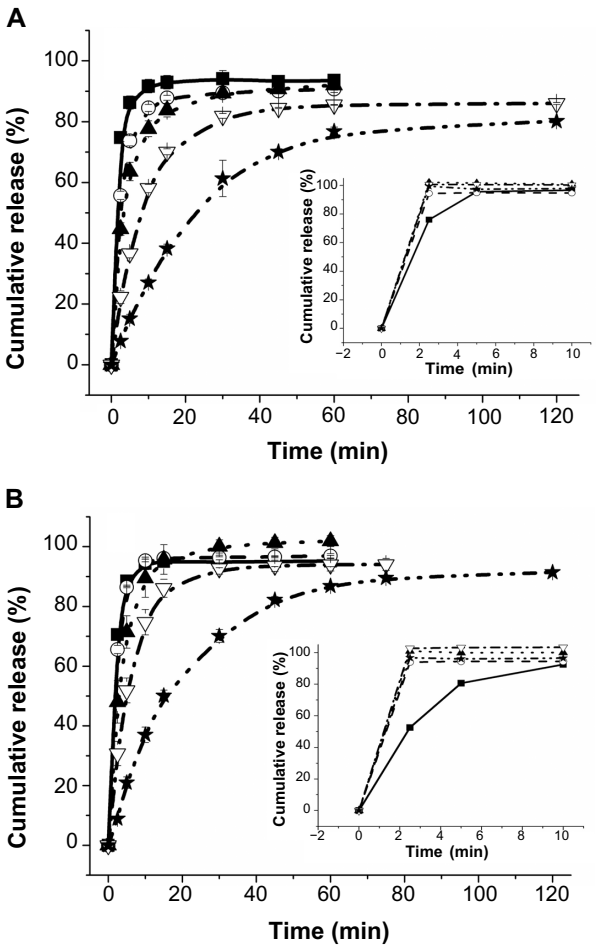

Figure 7 The release curves of drug-fiber complexes in pH 1.2 solution (**A**) and pH 6.8 buffer (**B**).
Notes: The small pictures in the lower right showed the release curves of drug powder. Atenolol (■, solid), Tramadol (○, dash), Venlafaxine (▲, dot), Sinomenine (▽, dash dot), Diltiazem (★, dash dot dot).

dose used was different in the two experiments (30 mg in this work and 120 mg in the previous report). Figure 9 shows the dissolution tests of three doses of diltiazem–fiber complexes. The drug release is irrelevant to the structure; the drug release is determined by the ionic reaction. The release of drug is also not due to the dissolution of drug

Table 5 The time after which 50% or 80% of the drug had been released from the fiber

Drug	$t_{50\%}$		$t_{80\%}$	
	pH 1.2 solution	pH 6.8 buffer	pH 1.2 solution	pH 6.8 buffer
Atenolol	1.6	1.7	3.3	3.4
Tramadol	2.1	1.8	7.4	4.0
Venlafaxine	3.0	2.7	11.1	6.9
Sinomenine	8.0	5.1	27.3	11.6
Diltiazem	22.0	15.0	119.0	41.9

Note: Unit of measurement: minutes.

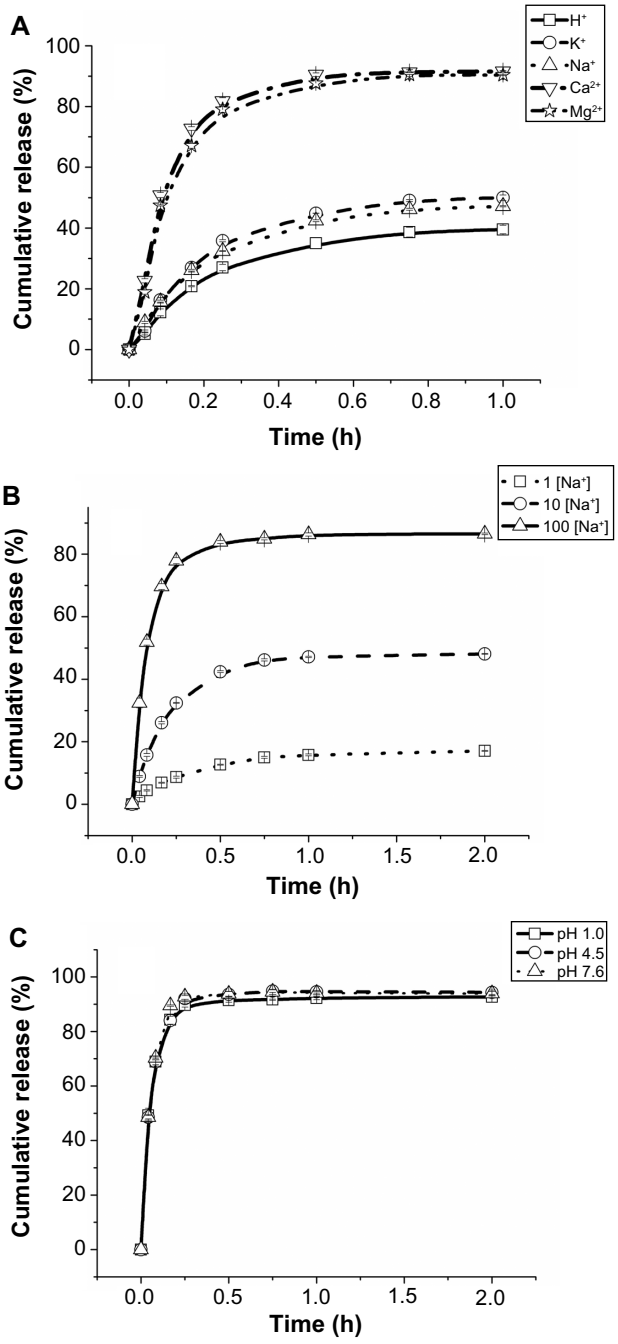

Figure 8 The release curves of venlafaxine-fiber complexes in different dissolution mediums.
Note: Different kinds of counter ions (**A**); different concentrations of counter ions (**B**); and different pH (**C**).

powder. Once the ionic reaction equilibrium was established between the drugs in fibers and that in release medium, the release was not continued though a good sink condition was maintained in release medium. As the dose decreased, the relative concentration of the extraction solution increased so as to shift the reaction toward drug release and make the release extent higher. Therefore, this dissolution method is

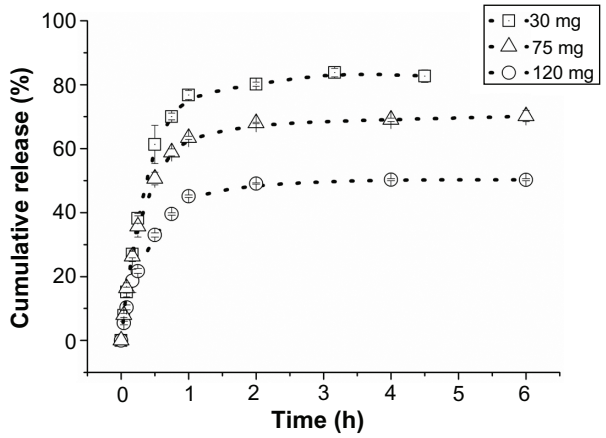

Figure 9 The release curves of diltiazem-fiber complexes in pH 1.2 solution with different doses (weighed equivalent to 30, 60 and 120 mg diltiazem hydrochloride).

more suitable for the release of small doses of drugs from ion-exchange fibers.

Conclusion

The load and release characteristics of model drugs with ion-exchange fibers was investigated in the present study to lay the groundwork for the application of ion-exchange fibers. Through the development of opposing exchange kinetics, ionic reaction was proved to be the rate-determining step for the loading process. Molecular weight was the most important influential factor for both drug load and release rate. Both of these decreased with increasing molecular weight, ie, a drug that loads quickly is released quickly too. pKa and the ring structure of drugs strengthened the affinity between the drug and fiber, while logP did not cause any profound differences. Different types and concentrations of counter ions or different amounts of complexes in the dissolution medium affect the release behavior, while pH is independent of it. These results could be very useful for predicting the load and release behavior of other drugs with ion-exchange fibers.

Acknowledgment

Financial support of the National Natural Science Foundation of China (No 81072603) is gratefully acknowledged.

Disclosure

The authors report no conflicts of interest in this work.

References

1. Helfferich F. *Ion Exchange*. New York, San Francisco, Toronto, London: McGraw-Hill Book Company; 1962.
2. Atyabi F, Sharma HL, Mohammad HA, Fell JT. Controlled drug release from coated floating ion exchange resin beads. *J Control Release*. 1996;42(1):25–28.
3. Xin C, Li-hong W, Jing Y, et al. Ketoconazole ion-exchange fiber complex: a novel method to reduce the individual difference of bioavailability in oral administration caused by gastric anacidity. *Pharm Dev Technol*. 2012;18(6):1346–1354.
4. Che X, Wang LH, Yang Y, et al. Ibuprofen ion-exchange fiber complex: improved dissolution and gastric tolerance based on ion exchange. *Drug Dev Ind Pharm*. 2013;39(5):744–751.
5. Yao H, Xu L, Han F, et al. A novel riboflavin gastro-mucoadhesive delivery system based on ion-exchange fiber. *Int J Pharm*. 2008;364(1):21–26.
6. Yu L, Li S, Yuan Y, Dai Y, Liu H. The delivery of ketoprofen from a system containing ion-exchange fibers. *Int J Pharm*. 2006;319(1–2):107–113.
7. Jaskari T, Vuorio M, Kontturi K, Urtti A, Manzanares JA, Hirvonen J. Controlled transdermal iontophoresis by ion-exchange fiber. *J Control Release*. 2000;67(2–3):179–190.
8. Xin C, Li-hong W, Yue Y, et al. A novel method to enhance the efficiency of drug transdermal iontophoresis delivery by using complexes of drug and ion-exchange fibers. *Int J Pharm*. 2012;428(1–2):68–75.
9. Xin C, Lihong W, Fei H, et al. To enhance the efficiency of nefopam transdermal iontophoresis by using a novel method based on ion-exchange fiber. *Drug Dev Ind Pharm*. 2014;40(1):9–16.
10. Jani R, Gan O, Ali Y, Rodstrom R, Hancock S. Ion exchange resins for ophthalmic delivery. *J Ocul Pharmacol*. 1994;10(1):57–67.
11. Chretien C, Boudy V, Allain P, Chaumeil JC. Indomethacin release from ion-exchange microspheres: impregnation with alginate reduces release rate. *J Control Release*. 2004;96(3):369–378.
12. Anand V, Kandarapu R, Garg S. Ion-exchange resins: carrying drug delivery forward. *Drug Discov Today*. 2001;6(17):905–914.
13. Hänninen K, Kaukonen AM, Kankkunen T, Hirvonen J. Rate and extent of ion-exchange process: the effect of physico-chemical characteristics of salicylate anions. *J Control Release*. 2003;91(3):449–463.
14. Ekman K. *Applied Radiation Processing of Polyolefins*. Turku, Finland: Åbo Akademi University; 1994.
15. Cortina JL, Warshawsky A, Kahana N, Kampel V, Sampaio CH, Kautzmann RM. Kinetics of goldcyanide extraction using ion-exchange resins containing piperazine functionality. *React Funct Polym*. 2003;54(1):25–35.
16. Lin LC, Juang RS. Ion-exchange kinetics of Cu(II) and Zn(II) from aqueous solutions with two chelating resins. *Chem Eng J*. 2007;132(1–3):205–213.
17. Chen L, Yang G, Zhang J. A study on the exchange kinetics of ion-exchange fiber. *React Funct Polym*. 1996;29(3):139–144.
18. Sujata AD, Banchero JT, White RR. Rates of ion exchange in the system Sodium-Potassium Dowex 50. *Ind Eng Chem*. 1955;47(10):2193–2199.
19. Abdekhodaie MJ, Wu XY. Drug loading onto ion-exchange microspheres: modeling study and experimental verification. *Biomaterials*. 2006;27(19):3652–3662.
20. Saiers JE, Hornberger GM, Liang L. First- and second-order kinetics approaches for modeling the transport of colloidal particles in porous media. *Water Resour Res*. 1994;30(9):2499–2506.
21. Debnath S, Ghosh UC. Kinetics, isotherm and thermodynamics for Cr(III) and Cr(VI) adsorption from aqueous solutions by crystalline hydrous titanium oxide. *J Chem Thermodyn*. 2008;40(1):67–77.
22. Fried V, Hameka HF, Blukis U. *Physical Chemistry*. New York: Macmillan Publishing Co, Inc.; 1975.
23. Wang WQ, Li MY, Zeng QX. Thermodynamics of Cr(VI) adsorption on strong alkaline anion exchange fiber. *Trans Nonferrous Met Soc China*. 2012;22(11):2831–2839.
24. Nollet H, Roels M, Lutgen P, Van der Meeren P, Verstraete W. Removal of PCBs from wastewater using fly ash. *Chemosphere*. 2003;53(6):655–665.
25. Borodkin S, Sundberg DP. Polycarboxylic acid ion-exchange resin adsorbates for taste coverage in chewable tablets. *J Pharmaceutical Sci*. 1971;60(10):1523–1527.

26. Wågberg L, Ödberg L, Lindström T, Aksberg R. Kinetics of adsorpton and ion-exchange reactions during adsorption of cationic polyelectrolytes onto cellulosic fibers. *J Colloid Interface Sci*. 1988;123(1):287–295.
27. Kressman TR, Kitchener JA. Cation exchange with a synthetic phenolsulphonate resin. Part III. Equilibria with large organic cations. *J Chem Soc*. 1949:1208–1210.
28. Prabhu NB, Marathe AS, Jain S, et al. Comparison of dissolution profiles for sustained release resinates of BCS class I drugs using USP Apparatus 2 and 4: a technical note. *AAPS Pharm Sci Tech*. 2008;9(3):769–773.